Agricultural and Forest Meteorology 268 (2019) 86–97

Contents lists available at ScienceDirect

Agricultural and Forest Meteorology

journal homepage: www.elsevier.com/locate/agrformet

Modeling impacts of mulching and climate change on crop production and N_2O emission in the Loess Plateau of China

Haixin Chen[a,b], Linchao Li[b], Xiaoqi Luo[b], Yi Li[b], De Li Liu[c,d], Ying Zhao[e], Hao Feng[a,b,*], Jia Deng[f,**]

[a] State Key Laboratory of Soil Erosion and Dryland Farming on the Loess Plateau, Northwest A&F University, Yangling, Shaanxi, 712100, China
[b] Institute of Water-saving Agriculture in Arid Areas of China, Northwest A&F University, Yangling, Shaanxi, 712100, China
[c] NSW Department of Primary Industries, Wagga Wagga Agricultural Institute, Wagga Wagga, NSW, 2650, Australia
[d] Climate Change Research Centre and ARC Centre of Excellence for Climate Extremes, University of New South Wales, Sydney, NSW, 2052, Australia
[e] College of Resources and Environmental Engineering, Ludong University, Yantai, Shandong, 264025, China
[f] Earth Systems Research Center, Institute for the Study of Earth, Oceans, and Space, University of New Hampshire, Durham, NH, 03824, USA

ARTICLE INFO

Keywords:
Crop yield
N_2O emission
Mulching
Climate change
Biogeochemical modeling

ABSTRACT

Covering soils using mulch can increase crop productivity in dryland agriculture. However, there remains large uncertainty regarding impacts of mulching on nitrous oxide (N_2O) emissions, especially under climate change (increases in air temperature and atmospheric CO_2 concentration and changes in precipitation). In this study, we applied a biogeochemical model, DeNitrification-DeComposition (DNDC), to predict impacts of different mulching practices on wheat (*Triticum aestivum* L.) and maize (*Zea mays* L.) yields and N_2O emissions under future climate scenarios in the South Loess Plateau of China. When tested against the observed crop yields and N_2O emissions under no-mulching (NM), straw mulching (SM), and plastic film mulching (PM), DNDC successfully simulated crop yields and annual N_2O emissions under all treatments. Simulations and observations both suggested that applying SM or PM increased crop yields and N_2O emissions in comparison with NM. Sensitivity analyses of crop yields and N_2O emissions indicated that the crop yields were primarily influenced by precipitation and N_2O emissions were sensitive to changes in air temperature, precipitation, soil organic carbon, and nitrogen application rate. Application of SM or PM reduced the sensitivity of the crop yield and N_2O emissions to precipitation change. Compared with historical climate conditions, future climate from 2017 to 2100 significantly increased crop yields except during the 2090s for NM or SM and during the 2070s to 2090s for PM under the high emission scenario (RCP8.5), while N_2O emissions were increased under all treatments. The positive impacts of PM on crop yields could be reduced under the RCP8.5 scenario. The DNDC predictions suggest that straw mulching might be an optimum mulching method to improve crop productivity and mitigate increasing N_2O under future climate conditions in semi-arid to sub-humid areas such as the South Loess Plateau of China.

1. Introduction

Nitrous oxide (N_2O) is an important greenhouse gas (GHG) with high global warming potential and long residence time in the atmosphere (Ciais et al., 2013). In addition, N_2O is a dominant anthropogenic, ozone-depleting gas, contributing to the depletion of stratospheric ozone (Ravishankara et al., 2009). The atmospheric concentration of N_2O has increased to 328 ppbv in 2016, and the increasing rate of N_2O concentration on a global scale has accelerated from 0.15 ppbv yr^{-1} 100 years ago to around 0.70 ppbv yr^{-1} at present (Smith, 2017). Globally, agriculture contributes about 59% of anthropogenic N_2O emissions, releasing 4.1 (uncertainty: 1.7 to 4.8) Tg (10^{12} g) N_2O-N per year (Ciais et al., 2013). Given the important role of agriculture in GHG emissions, agricultural ecosystems need to be managed by considering both their productivity and their environmental effects.

Mulching soil using natural or artificial materials has been extensively adopted in crop production, especially in relatively dry areas.

* Corresponding author at: State Key Laboratory of Soil Erosion and Dryland Farming on the Loess Plateau, Northwest A&F University, Yangling, Shaanxi, 712100, China.
** Corresponding author.
E-mail addresses: nercwsi@vip.sina.com (H. Feng), Jia.Deng@unh.edu (J. Deng).

https://doi.org/10.1016/j.agrformet.2019.01.002
Received 7 June 2018; Received in revised form 28 December 2018; Accepted 2 January 2019
Available online 16 January 2019
0168-1923/ © 2019 Elsevier B.V. All rights reserved.

Both straw and plastic film mulching practices have been shown to enhance crop productivity, due to the improvements in soil environments that are a result of modified soil temperature, reduced runoff and evaporation, and increased soil water availability (Dass and Bhattacharyya, 2017; Dong et al., 2018; Li et al., 2018; Zhang et al., 2018a). However, there remains large uncertainty regarding the impacts of straw and plastic film mulching on N_2O emissions. Previous studies have reported inconsistent impacts of applying straw mulching on N_2O emissions across different crop fields (e.g., Fracetto et al., 2017; Gomes et al., 2009; Jarecki et al., 2009; Lenka and Lal, 2013; Ma et al., 2009; Wu et al., 2018). Some studies have even obtained inconsistent results across different investigating years for a single crop field (Chen et al., 2017; Yagioka et al., 2015). Similarly, the effects of plastic film mulching on N_2O emissions were also variable, with increased (Arriaga et al., 2011; Cuello et al., 2015; Kim et al., 2017; Nishimura et al., 2012), unchanged (Liu et al., 2014), or decreased (Berger et al., 2013; Li et al., 2014; Yu et al., 2017) N_2O emissions observed after applying plastic film mulching. In addition, these previous studies were usually based on relatively short-term (1 month to 3 years) N_2O observations. Short-term studies may not be able to capture the long-term impacts of mulching (especially for straw) on crop growth and soil microbiological processes because the impacts could be variable under future climate changes that include increases in air temperature and atmospheric CO_2 concentration as well as changes in precipitation (Chen et al., 2017).

In addition to field measurements, modeling approaches have been applied to assess impacts of climate change or management practices on crop production and N_2O emissions in agricultural ecosystems. Process-based models are able to predict crop production and N_2O emissions under different management and environmental conditions by simulating comprehensive interactions of soil biogeochemical processes, crop growth, environmental factors, and anthropogenic activities (Abalos et al., 2016b). However, large uncertainty still exists in applying process-based models to evaluate impacts of mulching on crop yields and N_2O emissions because the models are often limited in representing different mulching treatments. Among these process-based models, the DeNitrification-DeComposition (DNDC) model has been extensively applied at both site and regional scales to predict carbon (C) and nitrogen (N) dynamics in different regions or countries (Gilhespy et al., 2014; Giltrap et al., 2010). Recently, a new module parameterizing plastic film mulching has been incorporated into DNDC (Han et al., 2014), and it has been applied to evaluate the effects of plastic film mulching on crop productivity, GHG emissions, and soil organic carbon (SOC) contents (Han et al., 2014; Yu et al., 2017, 2018; Zhang et al., 2017, 2018a). However, DNDC has not been applied to evaluate impacts of different mulching practices on crop yields and N_2O emissions yet.

The Loess Plateau of China has a typical semi-arid to sub-humid monsoon climate with limited precipitation and high evapotranspiration (Liu et al., 2009), and it is one of the areas in China most vulnerable to climate change (He et al., 2015). Air temperature has increased by 0.38 °C decade^{-1} during 1961 to 2010 in this area (Ding et al., 2016), which is around three times the rate of 0.13 °C decade^{-1} for the globally-averaged temperature increase (Flato et al., 2013). Annual total precipitation in this region has decreased in general from 1961 to 2010 (Wang et al., 2012). However, the decreasing trend was insignificant compared with inter-annual and spatial variability in precipitation (He et al., 2014). The future climate trend predicted from Global Climate Models (GCMs) generally showed much greater rates of increasing air temperature and large shifts in the precipitation distribution in this region although there remain large variations in both air temperature and precipitation across different GCMs (Flato et al., 2013; Liu et al., 2017b). In this study, we used 28 GCMs to predict the future climate in the South Loess Plateau of China and conducted DNDC-based long-term simulations to assess impacts of climate change on crop yields and N_2O emissions under different mulching practices. The objectives of this study were (1) to evaluate the performance of DNDC in simulating wheat and maize yields and N_2O emissions under no mulch, straw mulch, and plastic film mulch practices, (2) to quantify the sensitivities of crop yields and N_2O emissions to changes of key input parameters (i.e., air temperature, precipitation, soil clay content, SOC content, N application rate, and straw amount), and (3) to predict the impacts of different mulching practices on wheat and maize yields and N_2O emissions under future climate scenarios in the South Loess Plateau of China.

2. Materials and methods

2.1. Field site and experimental data

The field site was located in Yangling, Shaanxi Province, China (34°20′ N, 108°24′ E, 521 m a.s.l.). The field data used in this study were obtained at a crop field with the winter-wheat (*Triticum aestivum* L.) and summer-maize (*Zea mays* L.) rotation, which is a typical cropping system in the South Loess Plateau of China (Ding et al., 2018). The site has a semi-arid to sub-humid climate with a mean annual precipitation of 595 mm and an average air temperature of 13.9 °C from 1961 to 2010. The soil at the study field has a silty clay loam texture with 8% sand, 75% silt, and 17% clay in the top 10 cm layer (Chen et al., 2017). At the beginning of the experiment, the primary soil physical and chemical properties (0–20 cm) were bulk density 1.37 g cm^{-3}, pH (H_2O, 1:1) 8.20, field capacity 27.92% (volume/volume), wilting point 12.20% (volume/volume), SOC 8.14 g kg^{-1}, total soil nitrogen 0.95 g kg^{-1}, soil NO_3^--N 5.41 mg kg^{-1}, and soil NH_4^+-N 1.35 mg kg^{-1} (Chen et al., 2017).

The experimental data were obtained from October 2013 to September 2016. Three treatments were imposed in the experiment: NM (no straw or plastic film mulching), SM (straw mulching, soil surface was completely covered by wheat straw mulch at a rate of 4000 kg ha^{-1}) and PM (clear plastic film mulching, soil surface was completely covered by plastic film mulch). The treatments were replicated three times resulting in a total of nine plots that were fully randomized. Each plot was 5 m long and 2 m wide. Wheat was sown in October and harvested in early June of the next year, while maize was sown in June and harvested in September or October. The fertilizer and water applied were the same in all treatments. The application rates of N and P were 150 and 100 kg ha^{-1}, respectively, during the wheat growing seasons, and were 225 and 90 kg ha^{-1}, respectively, during the maize growing seasons. All plots received 30 mm of water through drip irrigation 1 or 2 times during each crop growing season. Details regarding the farming management practices (planting and harvest dates, tilling methods and depths, fertilizer types and amount, irrigation) can be found in Table S1 and Chen et al. (2017).

The N_2O flux data observed in this study were measured using the static chamber method. In general, a static chamber (50 × 50 × 50 cm) was sealed onto a bottom collar randomly installed into the soil between the wheat rows or maize plants in each plot. Gas samples were taken between 09:00 and 11:00 am every 10 days from October 2014 to September 2016. Nitrous oxide concentrations were analyzed using a gas chromatograph (Agilent 7890 A, Agilent Technologies, Inc., Santa Clara, USA). Gas fluxes were calculated from the rate of change of N_2O concentration, chamber volume, and soil surface area. Seasonal or annual total N_2O emissions were calculated by linear interpolation of the measured daily fluxes. The details regarding the measurements of the N_2O fluxes are described in the Supplementary Material file and by Chen et al. (2017).

2.2. The DNDC model

The DNDC (DeNitrification-DeComposition, version 9.5) model is a process-based biogeochemical model. The model was originally developed to predict N_2O emissions from U.S. agroecosystems (Li et al., 1992a, 1992b), and then has been expanded to simulate soil climate,

Table 1
Physiological parameters used for simulating crop growth with the DNDC model.

Parameters[a]	Winter-wheat	Summer-maize	Note
Maximum productivity under optimum growing conditions	3520	4000	kg C ha^{-1} y^{-1}
Biomass fractions at maturity	0.30/0.28/0.28/0.14	0.5/0.2/0.2/0.1	grain/leaf/stem/root
Biomass carbon to nitrogen ratio	86	44	–
Amount of nitrogen required for full growth	136	183	kg N ha^{-1} y^{-1}
TDD[b]	1200	2100	°C
Amount of water required by the crop to produce dry matter	180	120	g water/g dry matter
Optimum temperature for plant growth	25	32	°C
Index of biological nitrogen fixation	1.0	1.0	1.0 indicates no N-fixation

[a] parameter values were determined using previously published values or by calibrating the simulated crop yields against the field records in the first rotational year.
[b] the required cumulative air temperature heat sum above plant growth thresholds (-6 °C for wheat and 0 °C for maize) during the growing season (unit: °C d^{-1}) for full crop growth.

crop growth, and soil C and N dynamics in different ecosystems (e.g., Brilli et al., 2017; Gilhespy et al., 2014; Giltrap et al., 2010; Li et al., 2012; Zhang and Niu, 2016). DNDC is composed of two components. The first component includes the soil climate, crop growth, and decomposition sub-models, and is employed to predict crop growth and soil environmental factors (e.g., temperature, moisture, pH, redox potential, and substrate concentration). The second component includes nitrification, denitrification, and fermentation sub-models. This component simulates C and N transformations using the soil environmental factors that are predicted by the first component.

In DNDC, crop biomass is simulated by considering the effects of several environmental factors on crop growth, including radiation, air temperature, soil moisture, and N availability. Soil N dynamics are simulated through tracing a series of biogeochemical reactions: decomposition, microbial assimilation, plant uptake, ammonia volatilization, ammonium adsorption, nitrification, denitrification, and nitrate leaching. Nitrous oxide flux is predicted as either a by product or an intermediate product of nitrification and denitrification. DNDC has parameterized a set of farming management practices regulating soil environmental conditions and/or substrate concentrations, and thereby simulates the influence of management practices on crop growth and rates of C and N biogeochemical reactions. The model simulates the impacts of straw mulching on soil temperature and moisture based on straw amount primarily through parameterizing impacts on thermal properties of the surface soil layer and evaporation. In addition, straw mulching can influence soil organic C and N pools through additions of organic matter to the soil. Recently, DNDC has been improved by parameterizing plastic film mulching (Han et al., 2014). In DNDC, use of plastic film mulching directly influences soil temperature and moisture through regulation of several relevant processes (primarily heat transfer, runoff, and evapotranspiration) based on the area coverage and duration of the plastic film mulching (Han et al., 2014). Further details regarding the model structure and the physical, chemical, and biogeochemical processes incorporated into DNDC were described by Li (2000); Li et al. (2012); and Zhang et al. (2002).

2.3. Model test

The data required to run the DNDC model include daily meteorological data, soil properties, crop parameters, and farming management practices. In this study, daily meteorological data (maximum and minimum air temperature, and precipitation) from 2013 to 2016 were collected from a weather station located at the study site. Soil properties, including texture, clay fraction, bulk density, pH, field capacity, wilting point, hydrological conductivity, porosity, and SOC content, were determined through on-site measurements. More specifically, the soil texture, bulk density, hydrological conductivity, and SOC content were measured using the pipette, oven drying, falling-head, and potassium dichromate oxidation methods, respectively. The pH was measured using a compound glass electrode (Seven Easy Mettler Toledo, China). Field capacity and wilting point were determined using a 15 bar Pressure Plate Extractor (Model 1500F1, SoilMoisture Equipment Corp., Santa Barbara, CA, USA). The technique details regarding the measurements of these soil properties were described by Lu (2000) and Yi (2009). Farming management practices, including planting and harvest, tillage, fertilization, irrigation, straw and plastic film mulching, were determined based on local records. In order to simulate crop growth, DNDC requires several crop physiological parameters, including the maximum biomass production and its partitioning to shoot and root, the C/N ratio of plant material, the accumulative temperature for maturity, optimum temperature for growth, crop water demand, and an index of biological N fixation. Although DNDC provides default values for the crop parameters, it is recommended that these crop specific parameters be determined through local measurements or model calibration. We, therefore, estimated these parameters using previously published values or calibrating the simulated crop yields against the observed yields in the first rotational year from 2013 to 2014 (Table 1). After determining the crop parameters, DNDC was run for four years from 2013 to 2016. The simulations were compared against the measured soil temperature and soil moisture data, the crop yields of the second and third rotational years, and N_2O emissions (only available in the second and third rotational years) for model validation.

Two statistical indexes, the normalized root mean square error (*nRMSE*) and the coefficient of determination (R^2), were employed for quantitative comparisons. The *nRMSE* (Eq. (1)) can characterize the agreement between the simulations and field measurements, with the value of zero indicating no discrepancy. The R^2 examines the correlation between the simulations and field observations (Eq. (2)).

$$nRMSE = \sqrt{\frac{\sum_{i=1}^{n}(O_i - S_i)^2}{n}} \cdot \frac{100}{\bar{O}} \quad (1)$$

$$R^2 = \left(\frac{\sum_{i=1}^{n}(O_i - \bar{O})(S_i - \bar{S})}{\sqrt{\sum_{i=1}^{n}(O_i - \bar{O})^2 \sum_{i=1}^{n}(S_i - \bar{S})^2}} \right)^2 \quad (2)$$

where O_i and S_i are the observed and simulated values, $\bar{O}$ and $\bar{S}$ are their respective averages, and n is the number of values.

2.4. Sensitivity analysis

In order to determine the most important factors for regulating crop yields or N_2O emissions under different mulching conditions, we conducted a series of sensitivity tests using the DNDC model. The simulation of the rotation year October 2014 to October 2015 was selected as the baseline scenario. Alternative scenarios were constructed by changing a single input parameter by a fraction of -30% or +30% while keeping the other parameters unchanged. Six input parameters, including air temperature, precipitation, clay content, SOC content, N

application rate, and straw amount (for the SM treatment), were included in the sensitivity tests. The variation range of ± 30% was set to cover all or most of the observed variation in the six selected input parameters at the local study site. DNDC was run using the changed values for each selected input parameter, and the simulations of crop yield and N_2O emission were collected for a quantitative comparison. We used a sensitivity index (*SI*; Eq. (3)) to quantify the sensitivity of crop yield and N_2O emission to changes of the selected input factors (Deng et al., 2011; Li et al., 2006; Walker et al., 2000).

$$SI = \frac{(R_{max} - R_{min})/\bar{R}}{(P_{max} - P_{min})/\bar{P}} \quad (3)$$

where P_{min}, P_{max}, and $\bar{P}$ are the minimum, maximum, and average values of a given input parameter, respectively, and R_{min}, R_{max}, and $\bar{R}$ are the simulated results corresponding to P_{min}, P_{max}, and $\bar{P}$, respectively. Positive *SI* values suggest that the simulations are positively correlated to the given input parameters, while negative values suggest negative correlations. Higher absolute *SI* values indicate that the simulations are more sensitive to the given input parameters.

After identifying the most sensitive factors, we further investigated the responses of crop yield and N_2O emission to the changes in these factors using the Monte Carlo method. Specifically, we randomly changed a single input parameter ranging within a -30% to +30% range using the Monte Carlo method, while keeping the other parameters unchanged. In order to fully cover the variations of crop yield and N_2O emission, we created 800 scenarios by changing the value for each selected input factor. DNDC was run 800 times under these scenarios for each factor, and the simulations of crop yield and N_2O emission were collected for analysis.

2.5. Climate change scenarios

The representative concentration pathway (RCP) scenarios with medium-low (RCP4.5) and high (RCP8.5) emissions were employed to represent the future climate scenarios during 2017 to 2100. These two scenarios were selected because they more closely represent current socio-economic conditions of radiative forcing (4.5 and 8.5 W m^{-2} in 2100 for RCP4.5 and RCP8.5, respectively) and emissions (atmospheric CO_2 concentrations reaching 650 and 1370 ppm in 2100 for RCP4.5 and RCP8.5, respectively), and have more raw monthly GCM-projected data for statistically downscaling (Wang et al., 2015).

In order to cover uncertainties in the predicted future climate change, we used an ensemble of 28 GCMs that have been employed in many previously published climate impact studies (e.g., Anwar et al., 2015; Liu et al., 2017a; Ruan et al., 2018; Wang et al., 2015). Basic information for these 28 GCMs is presented in Table S2. Gridded fields of monthly average maximum and minimum air temperatures and monthly total precipitation at the study site during 1981 to 2100 were extracted from the GCM simulations under both RCP4.5 and RCP8.5 scenarios that are available in the World Climate Research Program's (WCRP's) Coupled Model Intercomparison Project phase 5 (CMIP5) dataset (https://cmip.llnl.gov/cmip5/; Taylor et al., 2012). To generate the daily climate data that are required by DNDC, we further downscaled the monthly climate data into daily climate data at the study site using the weather-generator-based statistically downscaled model (NWAI-WG) developed by Liu and Zuo (2012). Briefly, this downscaling process included two steps. The first step of spatial downscaling was to interpolate the gridded monthly GCM outputs to monthly values for the study site using an inverse distance-weighted (IDW) method, with a bias correction procedure applied (Liu and Zuo, 2012). The second step of temporal downscaling was to disaggregate the monthly data to daily data through the modified WGEN stochastic weather generator (Richardson and Wright, 1984). In addition, atmospheric CO_2 concentrations from 1981 to 2100 under RCP4.5 (Eq. (4)) and RCP 8.5 (Eq. (5)) scenarios were calculated by empirical functions as follows (Liu et al., 2017a; Ruan et al., 2018):

$$[CO_2]_{RCP4.5} = 650.18 + \frac{0.000075326y - 0.16276}{0.00022299 - 727.97y^2} - 0.00018747 \times (y - 2045)^3 \quad (4)$$

$$[CO_2]_{RCP8.5} = 1034.3 + \frac{267.78 - 1.6188y}{4.0143 + 53.342y^{-5.2882}} + 21.746 \times \left(\frac{y - 2020}{100}\right)^3 + 100.65 \times \left(\frac{y - 1911}{100}\right)^3 \quad (5)$$

where $[CO_2]$ is the atmospheric CO_2 concentration (ppm) in each year; y is the calendar year from1981–2100 (i.e., y = 1981, 1982, …, 2100).

In order to assess the long-term impacts of climate change and mulching practices on crop yields and N_2O emissions, the DNDC model was continuously run from 1981 to 2100 for the three treatments. We used local climate records for the period of 1981 to 2016 and downscaled climate projections of 28 GCMs under RCP4.5 and RCP8.5 for the period of 2017 to 2100. The rotational farming management practices from 1981 to 2100 were consistent with those recorded in the field records as being used for all treatments from 2014 to 2015. For all 168 simulations (28 GCMs × 2 climate scenarios × 3 treatments) under different climate and mulching practices, we calculated the simulated average crop yields and N_2O emissions during 2021 to 2040 (2030s), 2041 to 2060 (2050s), 2061 to 2080 (2070s), and 2081 to 2100 (2090s), and compared them with the corresponding simulations for 1981 to 2016 (the baseline period) with current climate conditions.

3. Results

3.1. Model evaluation

3.1.1. Crop yields

Modeled wheat and maize yields (Fig. 1) were in good agreement with observations during both the calibration (the first rotational year of 2013–2014) and validation (the second and third rotational years of 2014–2016) periods. The calculated *nRMSE* values across the three treatments ranged from 4.3% to 18.5% and 5.6% to 10.3%, respectively, for the wheat and maize calibration data set, and from 3.3% to 14.7% and 6.1% to 8.2%, respectively, for wheat and maize validation data set. DNDC also captured the impacts of drought and the mulch

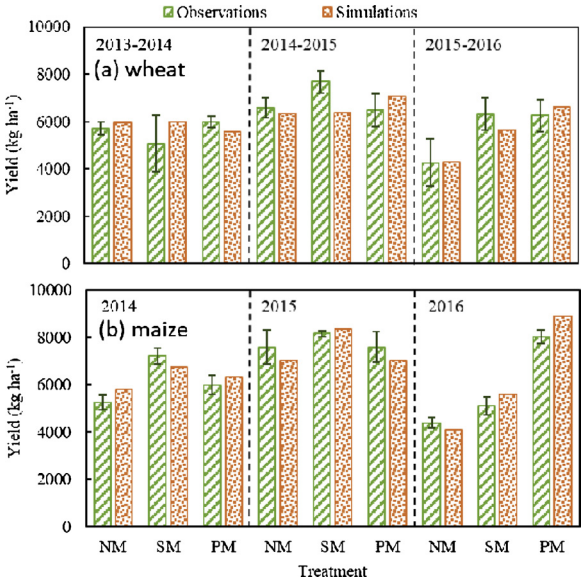

Fig. 1. Comparisons between simulated and observed yields of (a) winter-wheat and (b) summer-maize during the calibration (the first rotational year of 2013–2014) and validation (the second and third rotational years of 2014–2016) periods. Vertical bars indicate the standard deviations of three replications. NM: no-mulching, SM: straw mulching, PM: plastic film mulching.

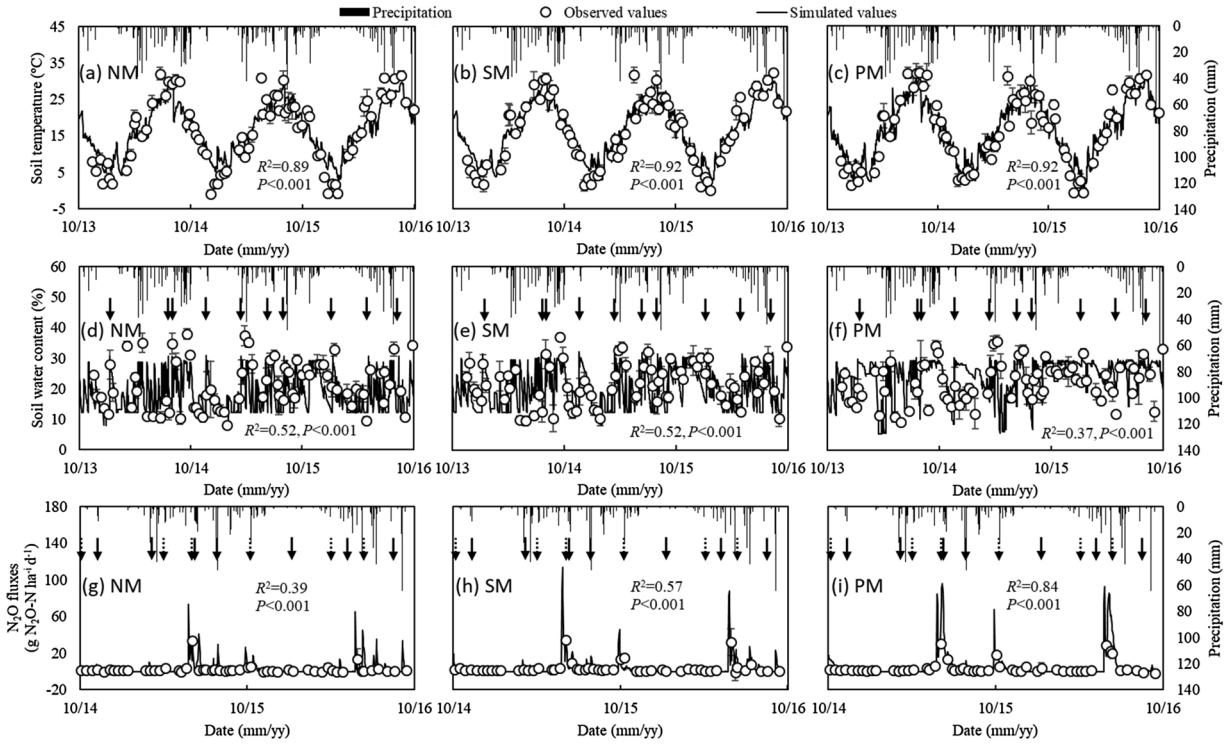

Fig. 2. Precipitation, and simulated and observed (a to c) soil temperature (5 cm), (d to f) soil water content (0–10 cm), and (g to i) N_2O fluxes. Vertical bars indicate the standard deviations of three replications. Solid arrows indicate the dates of irrigation applications, and dotted arrows indicate the dates of N fertilization events. NM: no-mulching, SM: straw mulching, PM: plastic film mulching.

covering on crop yield. The annual precipitation was 683, 533, and 494 mm, respectively, for the first, second, and third rotational year. Although annual precipitation was similar in both the second and third rotational years, precipitation distribution was more uneven in the third year. In that year, precipitation occurred primarily during the early and late wheat growing season, and often came as heavy, short-duration rainfall events during the maize growing season. Therefore, drought conditions resulted from the unevenly distributed precipitation. For the NM plots, both the model and field observations showed an obvious reduction in the wheat and maize yields as a result of drought in the third rotational year (Fig. 1). In comparison with NM, both the model and field observations indicated an increase in the crop yields under the SM and PM treatments in this third rotational year, primarily due to the increased crop water use efficiency under SM and PM. These results demonstrated that the DNDC model accurately predicted the crop yields under varied climate and mulch conditions at the study site.

3.1.2. Soil temperature and soil water content

The simulations of daily soil temperature (5 cm) were close to the measurements (Fig. 2a–c). The calculated statistical indices indicated that simulated soil temperatures were significantly correlated with the measurements in all three treatments (*nRMSE* range:16.9% to 23.8%; R^2 range: 0.88 to 0.92, P < 0.001; Fig. 2a–c and Table 2).

DNDC generally captured the temporal pattern and magnitude of the observed soil water content in the 0–10 cm layer (Fig. 2d–f), although there remained some obvious discrepancies for the PM treatment, especially during the periods with continuous drought (e.g., 11/2014 to 03/2015). The calculated *nRMSE* and R^2 varied from 19.3% to 26.3% and 0.37 to 0.52 ($P < 0.001$), respectively, across the three treatments (Table 2 and Fig. 2d–f). In addition, both the simulations and observations showed higher soil water content under SM and PM compared with NM (Table 2). Therefore, the model captured the observed positive impact of mulching resulting in greater soil water content.

Table 2
Simulated and observed soil temperature (5 cm), soil water content (0–10 cm), and annual N_2O emission.

Variables	*n*	Treatments	Average observations[a]	Average simulations[a]	*nRMSE* (%)
Soil temperature (°C)	76	NM	16.4	16.7	16.9
		SM	16.3	16.7	22.7
		PM	16.8	16.9	23.8
Soil water content (%)	76	NM	21.2	18.1	25.1
		SM	21.8	20.0	19.3
		PM	22.0	24.3	26.3
Annual N_2O emission (kg N_2O-N ha^{-1})	2	NM	0.72 ± 0.06	0.74	14.3
		SM	1.04 ± 0.04	1.10	13.3
		PM	1.14 ± 0.06	1.29	10.1

[a] averages (± standard deviation) from three replications.

3.1.3. Soil N_2O emissions

The N_2O flux measurements (Fig. 2g–i) showed similar seasonal patterns across the studied treatments, with high N_2O peaks occurring on days following N fertilizer application. In comparison with the measurements, DNDC generally captured the seasonal patterns of daily N_2O fluxes, although the magnitudes of some modeled N_2O peaks were higher than the field observations (e.g., the N_2O peaks following dates of base N fertilizer application during each maize growing season; Fig. 2g–i). The values of *nRMSE* and R^2 varied from 10.1% to 14.3% and 0.38 to 0.84 ($P < 0.001$), respectively, across the different treatments (Table 2 and Fig. 2g–i). In addition, DNDC successfully predicted the impacts of mulch on N_2O emissions. In comparison with NM, both the DNDC simulations and field observations indicated higher annual cumulative N_2O emissions for the SM and PM treatments (Table 2).

3.2. Sensitivity analysis

Table 3 summarizes the *SI* values for the selected input parameters.

Table 3
Calculated sensitivity indices (*SI*) quantifying the impacts of variations in selected input parameters on the simulated crop yields and N_2O emissions.

Input parameters	Baseline	Variation range	*SI* of crop yields			*SI* of N_2O emissions		
			NM	SM	PM	NM	SM	PM
Air temperature (°C)	14.4[a]	10.1-18.7	0.09	0.09	0.05	0.69	0.75	0.59
Precipitation (mm)	533[b]	373-693	1.08	0.78	0.59	0.71	0.26	0.33
Soil clay	0.17	0.12-0.22	0.11	0.40	0.37	0.16	0.30	0.18
SOC content (kg C kg^{-1})	0.008	0.006-0.010	0.01	0.03	0.02	0.80	0.94	0.58
N application rate (kg N ha^{-1} y^{-1})	375.0	262.5-487.5	0.01	0.25	0.36	0.69	0.84	0.95
Straw amount (kg ha^{-1} y^{-1})	8000	5600-10400	–	0.20	–	–	0.41	–

[a] average daily air temperature during the wheat-maize rotation from 10/2014 to 10/2015.
[b] annual total precipitation during the wheat-maize rotation from 10/2014 to 10/2015.

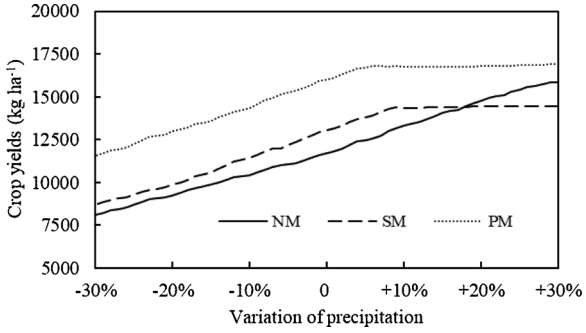

Fig. 3. Responses of simulated crop yields to change in precipitation. The crop yields are the sum of the simulated wheat and maize yields under different precipitations. NM: no-mulching, SM: straw mulching, PM: plastic film mulching.

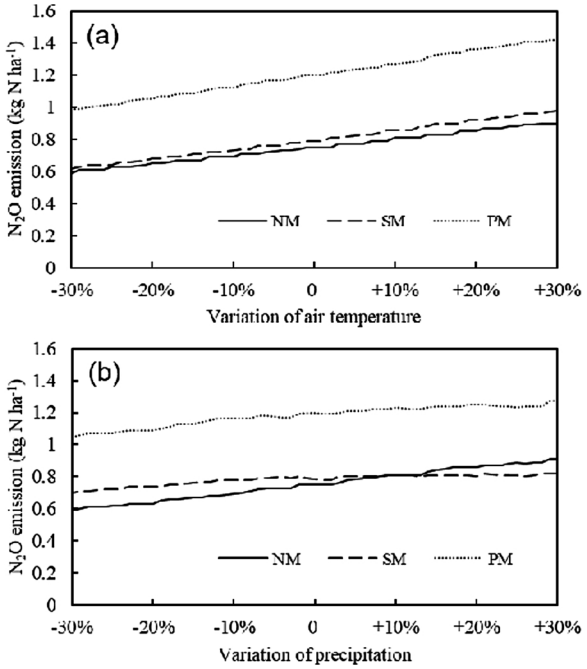

Fig. 5. Responses of N_2O emissions to change in (a) air temperature and (b) precipitation. NM: no-mulching, SM: straw mulching, PM: plastic film mulching.

For all three treatments, precipitation had a greater influence on crop yield than any other parameter, and the calculated *SI* for precipitation influence on yield ranked as NM > SM > PM. The sensitivity of crop yields to changes in precipitation is shown in Fig. 3. These results indicated that simulated crop yields increased linearly when the precipitation increased from -30% to +6%, with the rate of increase being similar among the treatments. However, the increasing trend stopped when the precipitation increased by around 6%, 9%, and 29% for PM, SM, and NM, respectively. These results indicated that the crop yield under NM was more sensitive to precipitation changes than under the other two mulch treatments when precipitation was +6% to +29% greater than the baseline precipitation amount.

Nitrous oxide emissions were very sensitive to variations in both SOC content and N application rate, with *SI* values ranging from 0.58 to 0.94 and 0.69 to 0.95, respectively, across the studied treatments (Table 3). Both SOC and N application rate exerted positive linear influences on N_2O emissions across the entire variation range for all three treatments (Fig. 4). In addition to SOC and N application rate, air temperature exerted a large influence on the N_2O emissions for all three studied treatments, and precipitation exerted a large influence on the N_2O emissions under NM (Table 3). Both air temperature and precipitation influenced N_2O emissions in a positive, linear manner for all three treatments (Fig. 5).

3.3. Future climate change and its impacts on crop yields and N_2O emissions

We summarized the projected climate data during the 2030s, 2050s, 2070s, and 2090s, and compared those values with the actual climate conditions from 1981 to 2016 (Fig. 6). The average maximum and

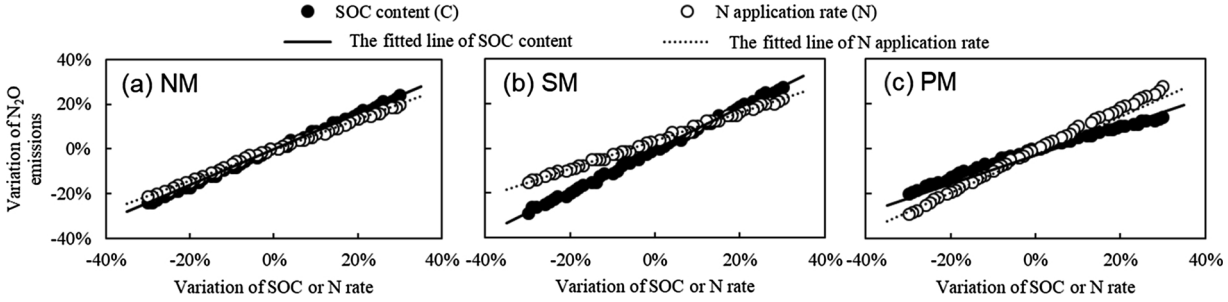

Fig. 4. Responses of N_2O emissions to change in SOC contents or N application rates. The lines represent the significant linear regression ($P < 0.001$). NM: no-mulching, SM: straw mulching, PM: plastic film mulching.

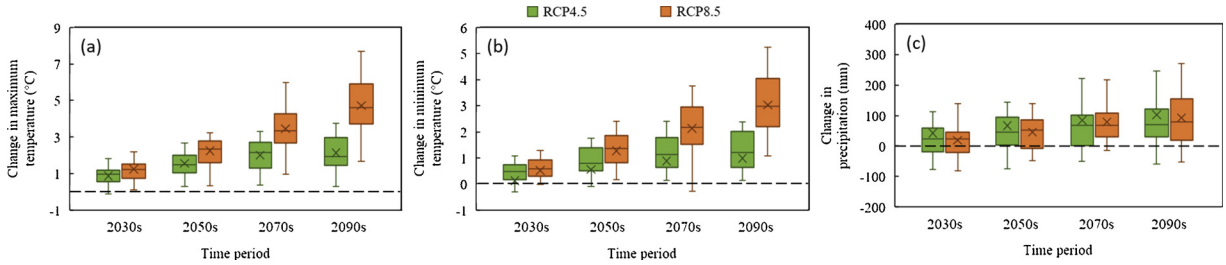

Fig. 6. Ensemble of 28 GCMs projected changes in annual average (a) maximum and (b) minimum temperature and (c) total precipitation under RCP4.5 and RCP8.5 scenarios at the study site in Yangling, Shaanxi Province, China. The changes are calculated for the four future time periods (2021–2040, 2041–2060, 2061–2080 and 2081–2100) over the baseline period (1981–2016, dotted lines). Each box summarizes 28 values. Box boundaries indicate the 25th and 75th percentiles; whiskers below and above the box indicate the 10th and 90th percentiles. Lines and crosses within each box indicate the median and mean, respectively.

minimum temperatures were 19.8 and 9.5 °C, respectively, and the average annual total precipitation was 584 mm (ranging from 331 to 958 mm) during 1981 to 2016. The projected temperature increased progressively with time (Fig. 6a and b). In comparison with the temperature during 1981 to 2016, the average maximum and minimum temperature in the 2090s increased by 2.1 and 1.0 °C, respectively, under RCP4.5, and by 4.7 and 3.0 °C, respectively, under RCP8.5. The projected precipitation increased as well (Fig. 6c). In comparison with the average annual precipitation during 1981 to 2016, the average annual precipitation increased by 43 and 19 mm for the 2030s, 67 and 45 mm for the 2050s, 84 and 79 mm for the 2070s, and 102 and 93 mm for the 2090s under RCP4.5 and RCP8.5, respectively.

Fig. 7a to c shows the simulated crop yields under the actual climate during 1981 to 2016 and the future climate in the 2030s, 2050s, 2070s, and 2090s. The average crop yields of NM and SM were projected to significantly ($P < 0.05$) increase in the future, except for the 2090s under RCP8.5 (Fig. 7a–b). The crop yields of PM significantly ($P < 0.05$) increased during the future periods from the 2030s to 2090s under RCP4.5, as compared with the crop yields during 1981 to 2016 (Fig. 7c). However, the increasing trend was only projected for the periods of the 2030s and 2050s under RCP8.5 (Fig. 7c). The average crop yield increases from 2021 to 2100 were 32.6%, 30.0%, and 9.7%, respectively, under RCP4.5, and 35.4%, 33.3%, and 6.2%, respectively, under RCP8.5 for the NM, SM, and PM treatments (Table 4). In comparison with NM, both SM and PM significantly ($P < 0.05$) increased the average crop yields from 2021 to 2100 under both RCP4.5 and RCP8.5 (Table 4). However, we noted that the positive impacts of PM on crop yields (compared with NM) were not observed during the 2070s to 2090s (Fig. 7a and c).

In comparison with the simulated N_2O emissions during 1981–2016, the possible future climate change would significantly ($P < 0.05$) increase the N_2O emissions for all three treatments (Fig. 7d–f). The average simulated N_2O emissions during 2021–2100 were increased by 50.5%, 80.7%, and 70.1%, respectively, for RCP4.5 and by 67.0%, 102.5%, and 86.8%, respectively, for RCP8.5 under NM, SM, and PM (Table 4). Under both RCP4.5 and RCP8.5, the predicted average N_2O emissions during 2021–2100 were significantly ($P < 0.05$) higher for both SM and PM treatments, as compared with NM (Table 4).

We further compared the yield-scaled N_2O emissions (i.e., the amount of N_2O emitted per unit of crop yield). The average predicted yield-scaled N_2O emissions during 2021–2100 were increased by 7.7% and 23.1% for NM, 38.5% and 30.4% for SM, and 30.4% and 76.9% for PM, respectively, under RCP4.5 and RCP8.5 scenarios, as compared with those during 1981–2016 (Table 4). In comparison with NM, both SM and PM significantly ($P < 0.05$) increased yield-scaled N_2O emissions under RCP4.5 and RCP8.5 (Table 4).

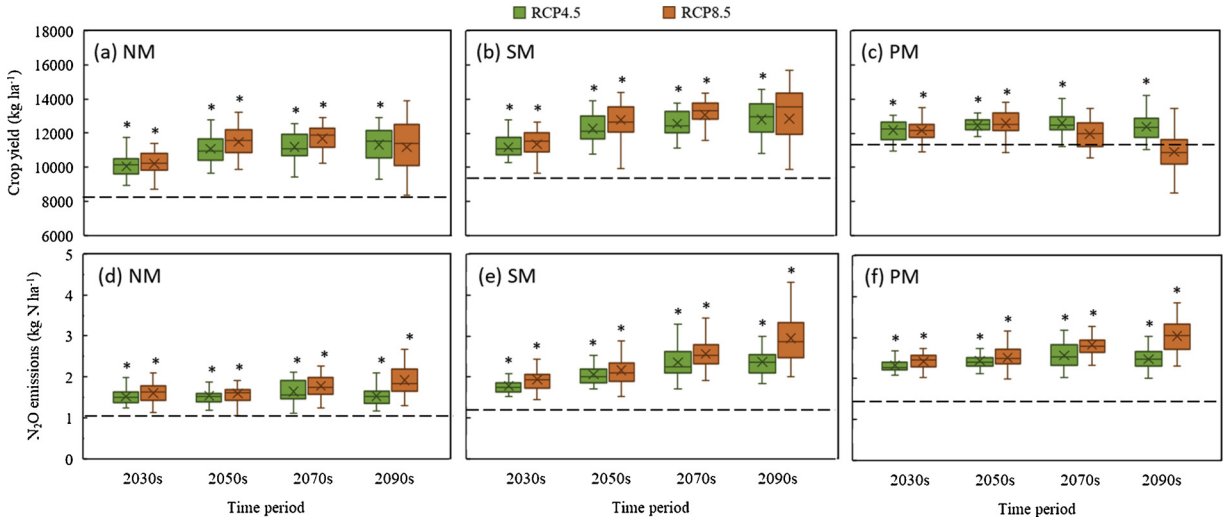

Fig. 7. Simulated (a to c) crop yields and (d to f) N_2O emissions during four future time periods (2021–2040, 2041–2060, 2061–2080 and 2081–2100) under RCP4.5 and RCP8.5 scenarios, as compared with the corresponding simulated crop yields and N_2O emissions during 1981–2016 (dotted lines). Each box summarizes 28 values of the DNDC simulated crop yields or N_2O emissions produced using 28 downscaled GCMs data. Box boundaries indicate the 25th and 75th percentiles; whiskers below and above the box indicate the 10th and 90th percentiles. Lines and crosses within each box indicate the median and mean, respectively. Asterisks (*) indicate significant differences against corresponding simulations during 1981–2016 ($P < 0.05$). NM: no-mulching, SM: straw mulching, PM: plastic film mulching.

Table 4
Comparison of simulated annual crop yields (kg ha^{-1}), cumulative N_2O emissions (kg N ha^{-1}) and yield-scaled N_2O emissions (g N kg^{-1} grain) under the actual climate during 1981–2016 and the future climate during 2021–2100 of RCP4.5 and RCP8.5 scenarios.

Treatments	1981-2016[a]			2021-2100 (RCP4.5)[b]			2021-2100 (RCP8.5)[c]		
	Crop yields	N_2O emissions	Yield-scaled N_2O emissions[d]	Crop yields	N_2O emissions	Yield-scaled N_2O emissions[d]	Crop yields	N_2O emissions	Yield-scaled N_2O emissions[d]
NM	8225 ± 2383C	1.03 ± 0.23B	0.13 ± 0.04A	10910 ± 635B	1.55 ± 0.19C	0.14 ± 0.02C	11133 ± 909C	1.72 ± 0.22C	0.16 ± 0.03C
SM	9389 ± 2187B	1.19 ± 0.18B	0.13 ± 0.03A	12203 ± 624A	2.15 ± 0.24B	0.18 ± 0.02B	12517 ± 1014A	2.41 ± 0.31B	0.20 ± 0.04B
PM	11313 ± 1813A	1.44 ± 0.53A	0.13 ± 0.05A	12407 ± 486A	2.45 ± 0.20A	0.20 ± 0.02A	11901 ± 497B	2.69 ± 0.27A	0.23 ± 0.03A

[a] data are mean ± SD over 35 years (n = 35). Different capital letters in a column indicate significant differences among treatments at $P < 0.05$ (LSD).
[b] and [c] data are mean ± SD over 28 GCMs (n = 28). Different capital letters in a column indicate significant differences among treatments at $P < 0.05$ (LSD).
[d] calculated by dividing the cumulative N_2O emissions by the annual crop yields.

4. Discussion

4.1. Model performance

4.1.1. Soil temperature and soil water content

In this study, the DNDC simulations of soil temperature and moisture (Fig. 2a–f and Table 2) were comparable with previous studies on simulating soil climate under film mulching (Han et al., 2014; Yu et al., 2017; Zhang et al., 2017). However, we noticed some discrepancies between the simulations and observations (e.g., 12/2015 to 03/2016; Fig. 2a–f). These discrepancies may partially result from the temporal inconsistency between the model outputs and field observations. DNDC reported outputs at a daily time step (Li et al., 1992a) while the observed soil temperature and soil water content were usually obtained from 9:00 am to 11:00 am on the gas sampling dates in this study. In particular, the temporal inconsistency may largely contribute to the under-prediction of soil moisture during some periods following rainfall (e.g., 09/2014, 04/2015; Fig. 2d–f). Because DNDC assumes that each rainfall event started at the beginning of the raining day and only reported the computed soil moisture at the end of the day (i.e., the reported soil moisture values are the results after simulating hydrologic processes, such as infiltration, soil evaporation and transpiration, among others), the high soil moisture measured in the field may be missed by the model's outputs at the end of the day (Deng et al., 2013). We also noticed that DNDC over-predicted soil moisture under PM during an event of continuous drought (11/2014-03/2015; Fig. 2f). This over-prediction was consistent with the result by Yu et al. (2017), who reported that DNDC over-estimated soil moisture under plastic film mulching in an arid region of China and attributed the discrepancies to the underestimations of plant growth and thereby transpiration. However, this reason may not be able to explain the overestimation of soil moisture in our study because the overestimation occurred in the early stages of wheat growth when plant transpiration was small. Therefore, it is possible that the overestimations in our study were due to the DNDC's under-prediction of soil evaporation under plastic film mulching that was also reported by Han et al. (2014).

4.1.2. Crop yields

DNDC employs a general crop growth module for different crop types, and crop growth is simulated at a daily time step by considering the impacts of several environmental factors on potential biomass production, including radiation, air temperature, soil moisture, and N availability (Zhang and Niu, 2016). Although this procedure was relatively weak in comparison with the existing plant models that are more mechanistic and usually parameterized for specific crop types (Chen et al., 2015; Zhang and Niu, 2016), the crop yield simulation by DNDC in this study (Fig. 1) was comparable to the performance of plant models with more detailed processes, such as CERES-Maize and CERES-Sorghum (Amouzou et al., 2018), CERES-Wheat (Nouri et al., 2017), EPIC (Zhang et al., 2018b), and APSIM (Li et al., 2016). In addition, DNDC captured the positive impacts of SM and PM on maintaining crop yields under drought conditions, although it was unable to simulate the yield maintenance in the second wheat growing season under SM (Fig. 1). In fact, impacts of using straw mulch on crop yield are still under dispute, with inconsistent conclusions across differing environments, due to the numerous factors and complex interactions that affect the microclimate and N cycle in fields with straw mulching (e.g., Chen et al., 2017; Ram et al., 2013; Stagnari et al., 2014; Wang et al., 2018; Yan et al., 2017, 2018). Because DNDC parameterizes empirical equations to adjust the soil microclimate conditions under straw mulching (Li, 2016), the discrepancies may be due to the differences between the model parameterization and actual influences in the studied field.

4.1.3. N_2O emissions

DNDC generally captured the seasonal dynamics of the observed N_2O emissions and the annual total N_2O emissions (Fig. 2g–i and Table 2). However, we noticed obvious discrepancies between the simulated and observed daily N_2O emissions (Fig. 2g–i). The DNDC performance in modeling N_2O emissions in our study was comparable with other DNDC testing studies that have reported good performance in simulating seasonal or annual N_2O emissions. However, those studies reported discrepancies in simulating daily N_2O fluxes (He et al., 2018; Smith et al., 2008; Ludwig et al., 2011; Zhang et al., 2016). The discrepancies in simulating daily N_2O fluxes could be partially due to the fact that the N_2O data for model testing were measured using manual static chambers. The manual chamber method is commonly used to measure GHG fluxes because it is relatively cheap and easy to operate in situ (Tallec et al., 2019). However, this method usually observes N_2O fluxes from limited spaces at relatively low temporal frequencies and thereby may miss hotspots and/or hot moments of N_2O fluxes (Fassbinder et al., 2013). For instance, daily N_2O fluxes were estimated using measurements between 09:00 am to 11:00 am and performed every 10 days in this study. This low measurement frequency may result in errors in representing the daily average N_2O fluxes (Chen et al., 2017) and cannot completely capture high N_2O fluxes that are often episodic, happening within 72 h of N fertilization or heavy rainfall events in agricultural soils (Fassbinder et al., 2013). Therefore, the discrepancies may partially result from the fact that the model predicted daily average N_2O fluxes using average daily climate and soil properties at a given site while the observations cannot accurately represent the average fluxes (Molina-Herrera et al., 2016). In addition, the observed seasonal or annual N_2O emissions may have been underestimated because the N_2O measurements using the manual static chambers may have missed some hotspots and/or hot moments of N_2O fluxes induced by events of heavy rainfall or farming management practices (Chen et al., 2017). The biases of the observed seasonal or annual N_2O emissions could also contribute to the discrepancies between the simulations and observations. Nevertheless, DNDC successfully captured the observed impacts of different mulching practices on N_2O emissions considering that the discrepancies between the simulated and observed annual N_2O emissions were relatively small (Table 2), the simulated daily N_2O fluxes significantly ($P < 0.001$)

correlated with the corresponding observations for all treatments (Fig. 2g–i), and the modeled impacts of mulching on N_2O emissions were consistent with the conclusion based on the field study (Chen et al., 2017). However, we note that the rigor of DNDC testing was hindered by the N_2O fluxes measured using the manual chamber method.

4.2. Sensitivity analysis

The results from the sensitivity analysis indicated that, of all the selected parameters, precipitation had the largest influence on crop yields among the selected parameters, with the precipitation influence being greatest for the NM treatment followed by SM and PM (Table 3). This suggested that the studied cropping system was water-limited, and both straw and plastic film mulching could be management options to mitigate the water-limiting effects on yield of the South Loess Plateau of China. Our study further demonstrated that the crop yields stopped increasing when precipitation reached 565 mm, 581 mm, and 688 mm under PM, SM, and NM, respectively (Fig. 3). The result was consistent with the evaluation by Zhang et al. (2018a), who concluded that areas with precipitation between 300 and 600 mm may be suitable for plastic film mulching in the Loess Plateau of China. The influence of N application rate on crop yields was greatest for the PM treatment followed by SM and NM in this study (Table 3), indicating that N was more important in straw or plastic film mulched systems where soil water was less limiting (Table 2). This conclusion was also in agreement with Qin et al. (2015), who reported significantly higher yields and N use efficiency (i.e., yield per unit N) by up to 60% in mulched cropping systems.

All of the tested input parameters, including air temperature, precipitation, clay content, SOC content, N application rate, and straw amount for SM showed noticeable influences on the N_2O emissions in this study (Table 3). Furthermore, the simulated N_2O emissions showed significantly linear ($P < 0.05$) increases due to increasing SOC content or N application rate (Fig. 4). Kim et al. (2013) proposed that the response of direct N_2O emissions to increasing of N application rate could be represented by three different phases – linear for N-limited soil conditions, exponential, or steady-state in C-limited soil conditions. In the linear phase, both plants and microbes compete for soil N, and N_2O emissions are primarily controlled by this competition for the soil available N. The studied cropping system appears to have been in this linear phase. Increasing SOC content could increase the availability of both dissolved organic carbon and substrates for nitrification and denitrification and favor the formation of anoxic micro-sites, and thereby increase N_2O emission (Ruser et al., 2006). Therefore, the simulated N_2O emissions increased along with increasing SOC. In addition, precipitation had a smaller influence on the N_2O emissions under SM or PM than NM (Table 3 and Fig. 5b), demonstrating that applying straw or plastic film mulching could offset the increases in N_2O emissions resulting from the increase in precipitation.

4.3. Climate change impacts on crop yields and N_2O emissions

In this study, we used statistically-downscaled data derived from 28 different GCMs to capture the uncertainty in future climate projections caused by uncertainty in the initial conditions, parameters, and model structure (Tebaldi and Knutti, 2007). We noticed large differences in forecast changes to precipitation among different GCMs (Fig. 6c), which may result from the GCMs themselves (such as different spatial resolution), statistically-downscaling method (such as bias correction), and the independence of selected GCMs (Wang et al., 2015). Despite large variations in the projected future climate across the 28 GCMs (Fig. 6), the average trends of increasing air temperature and precipitation were consistent with the results of Xu and Xu, (2012), who reported warming and wetting tendencies from 2011 to 2100 of 0.24 °C and 6.0% per decade, respectively, for RCP4.5, and 0.63 °C and 8.0% per decade, respectively, for RCP8.5 over China.

The impacts of climate change on crop yields were evaluated, and the results demonstrated that crop yields during 2021 to 2100 would likely be increased under all mulch treatments for both the RCP4.5 and RCP8.5 scenarios, except for PM, in which the projected yields during the 2070s to 2090s under RCP 8.5 were not significantly different from the baseline yields (Fig. 7a–c). The results were somewhat different from the previously published DNDC-based predictions regarding the impacts of climate change on crop yields in Northwest China. For example, Zhang et al. (2017) concluded that maize biomass constantly increased under both no-mulched and plastic film mulched conditions under future climate, and the increase was greater for the mulched than for the no-mulched treatments in the Northwest Loess Plateau of China. Yu et al. (2017) reported that lint yields were not changed in no-mulched conditions and significantly increased in plastic film mulched conditions under RCP2.6, RCP4.5, and RCP8.5 in the arid region of China. However, it should be noted that the baseline climate conditions in our study were different from those in these previous studies. These sites were generally much colder and drier than the studied site in our study, therefore the future warmer and wetter climate conditions would likely increase the crop (maize and lint) yields in these colder and drier regions (Yu et al., 2017; Zhang et al., 2017), while not providing additional beneficial growing conditions for wheat and maize production and yield during the 2070s to 2090s in the studied region, especially when using PM.

We also predicted different long-term impacts on the crop yields for different mulching practices. Although the significant ($P < 0.05$) impacts of improving crop productivity were predicted under SM and PM, as compared with NM, during both 1981 to 2016 (Fig. 7a–c) and the future period from 2021 to 2100 (Table 4), the positive impact of applying PM was projected to decrease along with climate change, and the simulated crop yields under PM were comparable with the yields under NM in the 2090s (Fig. 7a and c). These results suggested that climate could regulate impacts of mulching practices on crop growth, and therefore both current local climate conditions and future climate change need to be considered before applying mulching practices in semi-arid to sub-humid regions.

Compared with the predicted N_2O emissions during 1981–2016, the N_2O emissions significantly ($P < 0.05$) increased during 2021–2100 under both RCP4.5 and RCP8.5 scenarios for all three treatments (Fig. 7d–f and Table 4). These results were comparable with other studies in Europe (e.g., Abalos et al., 2016a; Abdalla et al., 2010) and in North America (e.g., Del Grosso and Parton, 2012; He et al., 2018; Smith et al., 2013; Tian et al., 2012). A future climate with warmer temperature and greater precipitation could positively or negatively affect N_2O emissions. On one hand, warmer temperature and greater precipitation could promote N_2O emissions by stimulating nitrification and/or denitrification (Abdalla et al., 2010; Yu et al., 2017). On the other hand, high atmospheric CO_2 concentrations could decrease soil water and N availability for N_2O production by increasing crop growth and crop water and N use efficiency (Kimball et al., 2002). In this study, the predicted N_2O emissions were greater under RCP8.5 than RCP4.5, indicating that the positive effects of future hydrothermal conditions on N_2O emissions were larger than the negative effects of increased CO_2 concentrations on N_2O emissions. In addition, we predicted significant ($P < 0.05$) greater N_2O emissions under SM or PM, as compared with NM, during 2021–2100 (Table 4). The predicted impacts of mulching practices on N_2O emissions under future climate conditions were consistent with the impacts under the current climate that were identified through the field study in the second rotational year (Chen et al., 2017). Furthermore, DNDC predicted the greatest N_2O emissions under PM for both current and future climate conditions. In comparison with NM or SM, the model predicted similar soil temperature and mineral N contents but greater soil water contents under PM. The average soil water contents (0–10 cm) under PM, SM, and NM were predicted as 24.8%, 20.0%, and 17.5%, respectively, for the current climate and 26.5%,

21.1%, and 18.7% for the future climate. Therefore, the greatest soil water contents were the primary reason for the predicted greatest N_2O emissions under PM at the study site.

Yield-scaled N_2O emissions, calculated by dividing the cumulative N_2O emissions by the crop yields, relate N_2O emissions to crop production (Abalos et al., 2016b). The average yield-scaled N_2O emissions during 2021–2100 were largely increased compared with those during 1981–2016, and the studied cropping system would likely emit more N_2O emissions per unit of grain under RCP8.5 than under RCP4.5 (Table 4). The amount of N_2O emitted per unit of crop yield ranked as NM < SM < PM for both future climate scenarios, and both NM and SM would likely significantly increase crop yields. Although PM can enhance crop yields under the current climate (Table 4) through increasing soil water contents (Table 2), its positive impact on the yields was projected to decrease along with climate change under RCP 8.5, and the wetter soil conditions under PM resulted in significantly greater average N_2O emissions and yield-scaled N_2O emissions during 2021–2100, as compared with NM or SM (Table 4). Therefore, both no-mulching and straw mulching may improve crop productivity, and offset the increases of N_2O emissions under projected future climate change in comparison with PM. Considering that straw mulching may increase crop yields and soil organic matter in comparison with NM and improve soil fertility by adding extra C and N into soil (Dong et al., 2018), straw mulching might be an optimum mulching method to improve food production and mitigate greenhouse gas emissions under future climate conditions.

In this study, we note that we did not consider other changes in social and other environmental factors as well as plant physiological characteristics and varieties, although these changes could affect both crop production and N_2O emissions. In particular, planting new crop cultivars or adaptation of crops to changed climate could offset some negative climate change impacts on crop production (He et al., 2018; Smith et al., 2013). Xiao and Tao (2014) suggested that wheat yield increases from 1980 to 2009 were largely due to newer cultivars and improvements in farming management practices in the North China Plain, although climate change exerted large impacts on wheat yield as well. Changes in varieties, plant species, or community composition may also affect aboveground and belowground plant productivity as well as ecosystem function (Elmendorf et al., 2015; Harte et al., 2015; Liu et al., 2018). In addition, future changes in farming management practices could affect N_2O emission. For example, using legumes in a rotational cropping system could reduce yield-scaled N_2O emissions under future climate change (Li et al., 2017; Ma et al., 2018). Considering that changes in social factors, farming management practices, crop physiological characteristics, and varieties may significantly affect crop production and N_2O emissions, further research is needed to evaluate the impacts of these changes on crop yield and N_2O emissions.

5. Conclusions

This study tested DNDC against the observed crop yields and N_2O emissions from a typical cropping system (winter-wheat and summer-maize rotation) in the South Loess Plateau of China under the treatments of no-mulching, straw mulching, and plastic film mulching. The model tests indicated that DNDC was capable of predicting the crop yields and annual total N_2O emissions under the different mulching treatments. Both the simulations and field observations showed positive impacts of SM or PM on increasing crop yields and N_2O emissions under current climate conditions. The results from the sensitivity analyses indicated that the crop yields were primarily influenced by precipitation. Air temperature, SOC content, and N application rate exerted relatively large impacts on the N_2O emissions for all three treatments, while precipitation showed large impacts only for NM. The impacts of climate change on crop yields and N_2O emissions under different mulching practices were simulated with DNDC. These long-term simulations demonstrated that 1) crop yields would likely be increased under all of the treatments except for PM, in which the yields under the current climate were not significantly different from the yields in the 2070s and 2090s under RCP8.5; 2) N_2O emissions would likely be increased for all of the treatments; and 3) the positive impacts of PM on crop yields could be reduced in response to climate change under the RCP8.5 scenario. These results suggest that straw mulching might be an optimum mulching method to improve crop production and to mitigate N_2O increases under future climate conditions in semi-arid to sub-humid areas such as the South Loess Plateau of China.

Acknowledgments

We thank two anonymous reviewers and editors for their constructive comments. This work was jointly supported by the National Natural Science Foundation of China (41807328, 51879224), the National 863 Research Program (2013AA102904), the 111 Project (B12007), the China Postdoctoral Science Foundation (2018M643752), and the Technology Co-innovation Project in Shaanxi Province (2016KTZDNY03-06). The senior author acknowledges that the China Scholarship Council provided the scholarship and University of New Hampshire provided office facilities for conducting this work.

In memory of Prof. Changsheng Li, we especially appreciate him for his enthusiasm and dedication to the DNDC study and education.

Appendix A. Supplementary data

Supplementary material related to this article can be found, in the online version, at doi:https://doi.org/10.1016/j.agrformet.2019.01.002.

References

Abalos, D., Cardenas, L.M., Wu, L., 2016a. Climate change and N_2O emissions from South West England grasslands: a modelling approach. Atmos. Environ. 132, 249–257.

Abalos, D., Smith, W.N., Grant, B.B., Drury, C.F., MacKell, S., Wagner-Riddle, C., 2016b. Scenario analysis of fertilizer management practices for N_2O mitigation from corn systems in Canada. Sci. Total Environ. 573, 356–365.

Abdalla, M., Jones, M., Williams, M., 2010. Simulation of N_2O fluxes from Irish arable soils: effect of climate change and management. Biol. Fert. Soils 46 (3), 247–260.

Amouzou, K.A., Naab, J.B., Lamers, J.P.A., Becker, M., 2018. CERES-Maize and CERES-Sorghum for modeling growth, nitrogen and phosphorus uptake, and soil moisture dynamics in the dry savanna of West Africa. Field Crop. Res. 217, 134–149.

Anwar, M.R., Liu, D.L., Farquharson, R., Macadam, I., Abadi, A., Finlayson, J., Wang, B., Ramilan, T., 2015. Climate change impacts on phenology and yields of five broadacre crops at four climatologically distinct locations in Australia. Agric. Syst. 132, 133–144.

Arriaga, H., Núñez-Zofío, M., Larregla, S., Merino, P., 2011. Gaseous emissions from soil biodisinfestation by animal manure on a greenhouse pepper crop. Crop Prot. 30 (4), 412–419.

Berger, S., Kim, Y., Kettering, J., Gebauer, G., 2013. Plastic mulching in agriculture - friend or foe of N_2O emissions? Agric. Ecosyst. Environ. 167, 43–51.

Brilli, L., Bechini, L., Bindi, M., Carozzi, M., Cavalli, D., Conant, R., Dorich, C.D., Doro, L., Ehrhardt, F., Farina, R., Ferrise, R., Fitton, N., Francaviglia, R., Grace, P., Iocola, I., Klumpp, K., Leonard, J., Martin, R., Massad, R.S., Recous, S., Seddaiu, G., Sharp, J., Smith, P., Smith, W.N., Soussana, J.-F., Bellocchi, G., 2017. Review and analysis of strengths and weaknesses of agro-ecosystem models for simulating C and N fluxes. Sci. Total Environ. 598, 445–470.

Chen, H., Zhao, Y., Feng, H., Li, H., Sun, B., 2015. Assessment of climate change impacts on soil organic carbon and crop yield based on long-term fertilization applications in Loess Plateau. China. Plant Soil 390 (1-2), 401–417.

Chen, H., Liu, J., Zhang, A., Chen, J., Cheng, G., Sun, B., Pi, X., Dyck, M., Si, B., Zhao, Y., Feng, H., 2017. Effects of straw and plastic film mulching on greenhouse gas, emissions in Loess Plateau, China: a field study of 2 consecutive wheat-maize rotation cycles. Sci. Total Environ. 579, 814–824.

Ciais, P., Sabine, C., Bala, G., Bopp, L., Brovkin, V., Canadell, J., Chhabra, A., DeFries, R., Galloway, J., Heimann, M., Jones, C., Le Quéré, C., Myneni, R.B., Piao, S., Thornton, P., 2013. Carbon and other biogeochemical cycles. In: Stocker, T.F., Qin, D., Plattner, G.-K., Tignor, M., Allen, S.K., Boschung, J., Nauels, A., Xia, Y., Bex, V., Midgley, P.M. (Eds.), Climate Change 2013: The Physical Science Basis. Contribution of Working Group I to the Fifth Assessment Report of the Intergovernmental Panel on Climate Change. Cambridge University Press, Cambridge, United Kingdom and New York, NY, USA, pp. 465–570.

Cuello, J.P., Hwang, H.Y., Gutierrez, J., Kim, S.Y., Kim, P.J., 2015. Impact of plastic film mulching on increasing greenhouse gas emissions in temperate upland soil during maize cultivation. Appl. Soil Ecol. 91, 48–57. https://doi.org/10.1016/j.apsoil.2015.02.007.

Dass, A., Bhattacharyya, R., 2017. Wheat residue mulch and anti-transpirants improve productivity and quality of rainfed soybean in semi-arid north-Indian plains. Field Crop. Res. 210, 9–19.
Del Grosso, S.J., Parton, W.J., 2012. Climate change increases soil nitrous oxide emissions. New Phytol. 196 (2), 327–328.
Deng, J., Zhu, B., Zhou, Z., Zheng, X., Li, C., Wang, T., Tang, J., 2011. Modeling nitrogen loadings from agricultural soils in southwest China with modified DNDC. J. Geophys. Res. (G2), 116.
Deng, J., Zhou, Z., Zheng, X., Li, C., 2013. Modeling impacts of fertilization alternatives on nitrous oxide and nitric oxide emissions from conventional vegetable fields in southeastern China. Atmos. Environ. 81, 642–650.
Ding, D.Y., Feng, H., Zhao, Y., He, J.Q., Zou, Y.F., Jin, J.M., 2016. Modifying winter wheat sowing date as an adaptation to climate change on the Loess Plateau. Agron. J. 108 (1), 53–63.
Ding, D., Zhao, Y., Feng, H., Hill, R.L., Chu, X., Zhang, T., He, J., 2018. Soil water utilization with plastic mulching for a winter wheat-summer maize rotation system on the Loess Plateau of China. Agric. Water Manage. 201, 246–257.
Dong, Q.G., Yang, Y., Yu, K., Feng, H., 2018. Effects of straw mulching and plastic film mulching on improving soil organic carbon and nitrogen fractions, crop yield and water use efficiency in the Loess Plateau. China. Agric. Water Manage. 201, 133–143.
Elmendorf, S.C., Henry, G.H.R., Hollister, R.D., Fosaa, A.M., Gould, W.A., Hermanutz, L., Hofgaard, A., Jónsdóttir, I.S., Jorgenson, J.C., Lévesque, E., Magnusson, B., Molau, U., Myers-Smith, I.H., Oberbauer, S.F., Rixen, C., Tweedie, C.E., Walker, M.D., 2015. Experiment, monitoring, and gradient methods used to infer climate change effects on plant communities yield consistent patterns. Proc. Natl. Acad. Sci. U. S. A. 112 (2), 448–452.
Fassbinder, J.J., Schultz, N.M., Baker, J.M., Griffis, T.J., 2013. Automated, low-power chamber system for measuring nitrous oxide emissions. J. Environ. Qual. 42 (2), 606–614.
Flato, G., Marotzke, J., Abiodun, B., Braconnot, P., Chou, S.C., Collins, W., Cox, P., Driouech, F., Emori, S., Eyring, V., Forest, C., Gleckler, P., Guilyardi, E., Jakob, C., Kattsov, V., Reason, C., Rummukainen, M., 2013. Evaluation of climate models. In: Stocker, T.F., Qin, D., Plattner, G.-K., Tignor, M., Allen, S.K., Boschung, J., Nauels, A., Xia, Y., Bex, V., Midgley, P.M. (Eds.), Climate Change 2013: The Physical Science Basis. Contribution of Working Group I to the Fifth Assessment Report of the Intergovernmental Panel on Climate Change. Cambridge University Press, Cambridge, United Kingdom and New York, NY, USA, pp. 741–866.
Fracetto, F.J.C., Fracetto, G.G.M., Bertini, S.C.B., Cerri, C.C., Feigl, B.J., Siqueira Neto, M., 2017. Effect of agricultural management on N_2O emissions in the Brazilian sugarcane yield. Soil Biol. Biochem. 109, 205–213.
Gilhespy, S.L., Anthony, S., Cardenas, L., Chadwick, D., del Prado, A., Li, C., Misselbrook, T., Rees, R.M., Salas, W., Sanz-Cobena, A., Smith, P., Tilston, E.L., Topp, C.F.E., Vetter, S., Yeluripati, J.B., 2014. First 20 years of DNDC (DeNitrification DeComposition): model evolution. Ecol. Modell. 292, 51–62.
Giltrap, D.L., Li, C., Saggar, S., 2010. DNDC: a process-based model of greenhouse gas fluxes from agricultural soils. Agric. Ecosyst. Environ. 136 (3), 292–300.
Gomes, J., Bayer, C., de Souza Costa, F., de Cassia Piccolo, M., Zanatta, J.A., Vieira, F.C.B., Six, J., 2009. Soil nitrous oxide emissions in long-term cover crops-based rotations under subtropical climate. Soil Tillage Res. 106 (1), 36–44.
Han, J., Jia, Z., Wu, W., Li, C., Han, Q., Zhang, J., 2014. Modeling impacts of film mulching on rainfed crop yield in Northern China with DNDC. Field Crop. Res. 155, 202–212.
Harte, J., Saleska, S.R., Levy, C., 2015. Convergent ecosystem responses to 23-year ambient and manipulated warming link advancing snowmelt and shrub encroachment to transient and long-term climate–soil carbon feedback. Glob. Change Biol. 21 (6), 2349–2356. https://doi.org/10.1111/gcb.12831.
He, L., Cleverly, J., Chen, C., Yang, X., Li, J., Liu, W., Yu, Q., 2014. Diverse responses of winter wheat yield and water use to climate change and variability on the Semiarid Loess Plateau in China. Agron. J. 106 (4), 1169–1178.
He, L., Asseng, S., Zhao, G., Wu, D., Yang, X., Zhuang, W., Jin, N., Yu, Q., 2015. Impacts of recent climate warming, cultivar changes, and crop management on winter wheat phenology across the Loess Plateau of China. Agric. For. Meteorol. 200, 135–143.
He, W., Yang, J.Y., Drury, C.F., Smith, W.N., Grant, B.B., He, P., Qian, B., Zhou, W., Hoogenboom, G., 2018. Estimating the impacts of climate change on crop yields and N_2O emissions for conventional and no-tillage in Southwestern Ontario, Canada. Agric. Syst. 159, 187–198.
Jarecki, M.K., Parkin, T.B., Chan, A.S., Kaspar, T.C., Moorman, T.B., Singer, J.W., Kerr, B.J., Hatfield, J.L., Jones, R., 2009. Cover crop effects on nitrous oxide emission from a manure-treated Mollisol. Agric. Ecosyst. Environ. 134 (1-2), 29–35.
Kim, D.G., Hernandez-Ramirez, G., Giltrap, D., 2013. Linear and nonlinear dependency of direct nitrous oxide emissions on fertilizer nitrogen input: a meta-analysis. Agric. Ecosyst. Environ. 168, 53–65.
Kim, G.W., Das, S., Hwang, H.Y., Kim, P.J., 2017. Nitrous oxide emissions from soils amended by cover-crops and under plastic film mulching: fluxes, emission factors and yield-scaled emissions. Atmos. Environ. 152, 377–388.
Kimball, B.A., Kobayashi, K., Bindi, M., 2002. Responses of agricultural crops to Free-air CO_2 enrichment. In: Sparks, D.L. (Ed.), Adv. Agron. Academic Press, pp. 293–368.
Lenka, N.K., Lal, R., 2013. Soil aggregation and greenhouse gas flux after 15 years of wheat straw and fertilizer management in a no-till system. Soil Tillage Res. 126, 78–89.
Li, C., 2000. Modeling trace gas emissions from agricultural ecosystems. Nutr. Cycling Agroecosyst. 58 (1-3), 259–276.
Li, C., 2016. Biogeochemistry: Scientific Fundamentals and Modeling Approach. Tsinghua University Press, Beijing, China (in Chinese).
Li, C., Frolking, S., Frolking, T.A., 1992a. A model of nitrous oxide evolution from soil driven by rainfall events: 1. Model structure and sensitivity. J. Geophys. Res. D: Atmos. 97 (D9), 9759–9776.
Li, C., Frolking, S., Frolking, T.A., 1992b. A model of nitrous oxide evolution from soil driven by rainfall events: 2. Model applications. J. Geophys. Res. D: Atmos. 97 (D9), 9777–9783.
Li, C., Farahbakhshazad, N., Jaynes, D.B., Dinnes, D.L., Salas, W., McLaughlin, D., 2006. Modeling nitrate leaching with a biogeochemical model modified based on observations in a row-crop field in Iowa. Ecol. Modell. 196 (1), 116–130.
Li, C., Salas, W., Zhang, R., Krauter, C., Rotz, A., Mitloehner, F., 2012. Manure-DNDC: a biogeochemical process model for quantifying greenhouse gas and ammonia emissions from livestock manure systems. Nutr. Cycling Agroecosyst. 93 (2), 163–200.
Li, Z., Zhang, R., Wang, X., Chen, F., Lai, D., Tian, C., 2014. Effects of plastic film mulching with drip irrigation on N_2O and CH_4 emissions from cotton fields in arid land. J. Agric. Sci. 152 (4), 534–542.
Li, J., Wang, E., Wang, Y., Xing, H., Wang, D., Wang, L., Gao, C., 2016. Reducing greenhouse gas emissions from a wheat-maize rotation system while still maintaining productivity. Agric. Syst. 145, 90–98.
Li, Y., Liu, D.L., Schwenke, G., Wang, B., Macadam, I., Wang, W.J., Li, G.D., Dalal, R., 2017. Responses of nitrous oxide emissions from crop rotation systems to four projected future climate change scenarios on a black Vertosol in subtropical Australia. Clim. Change 142 (3), 545–558.
Li, Z., Lai, X., Yang, Q., Yang, X., Cui, S., Shen, Y., 2018. In search of long-term sustainable tillage and straw mulching practices for a maize-winter wheat-soybean rotation system in the Loess Plateau of China. Field Crop. Res. 217, 199–210.
Liu, C.A., Jin, S.L., Zhou, L.M., Jia, Y., Li, F.M., Xiong, Y.C., Li, X.G., 2009. Effects of plastic film mulch and tillage on maize productivity and soil parameters. Eur. J. Agron. 31 (4), 241–249.
Liu, J., Zhu, L., Luo, S., Bu, L., Chen, X., Yue, S., Li, S., 2014. Response of nitrous oxide emission to soil mulching and nitrogen fertilization in semi-arid farmland. Agric. Ecosyst. Environ. 188, 20–28.
Liu, D.L., Zeleke, K.T., Wang, B., Macadam, I., Scott, F., Martin, R.J., 2017a. Crop residue incorporation can mitigate negative climate change impacts on crop yield and improve water use efficiency in a semiarid environment. Eur. J. Agron. 85, 51–68.
Liu, J., Du, H., Wu, Z., He, H.S., Wang, L., Zong, S., 2017b. Recent and future changes in the combination of annual temperature and precipitation throughout China. Int. J. Clim. 37 (2), 821–833.
Liu, H., Mi, Z., Lin, L., Wang, Y., Zhang, Z., Zhang, F., Wang, H., Liu, L., Zhu, B., Cao, G., Zhao, X., Sanders, N.J., Classen, A.T., Reich, P.B., He, J.-S., 2018. Shifting plant species composition in response to climate change stabilizes grassland primary production. Proc. Natl. Acad. Sci. U. S. A. 115 (16), 4051–4056.
Liu, D.L., Zuo, H., 2012. Statistical downscaling of daily climate variables for climate change impact assessment over New South Wales, Australia. Clim. Change 115 (3-4), 629–666.
Lu, R.K., 2000. Methods of Soil and Agro-chemical Analysis. China Agricultural Science and Technology Press, Beijing, China (in Chinese).
Ludwig, B., Bergstermann, A., Priesack, E., Flessa, H., 2011. Modelling of crop yields and N_2O emissions from silty arable soils with differing tillage in two long-term experiments. Soil Tillage Res. 112 (2), 114–121.
Ma, J., Ma, E., Xu, H., Yagi, K., Cai, Z., 2009. Wheat straw management affects CH_4 and N_2O emissions from rice fields. Soil Biol. Biochem. 41 (5), 1022–1028.
Ma, Y., Schwenke, G., Sun, L., Liu, D.L., Wang, B., Yang, B., 2018. Modeling the impact of crop rotation with legume on nitrous oxide emissions from rain-fed agricultural systems in Australia under alternative future climate scenarios. Sci. Total Environ. 630, 1544–1552.
Molina-Herrera, S., Haas, E., Klatt, S., Kraus, D., Augustin, J., Magliulo, V., Tallec, T., Ceschia, E., Ammann, C., Loubet, B., Skiba, U., Jones, S., Brümmer, C., Butterbach-Bahl, K., Kiese, R., 2016. A modeling study on mitigation of N_2O emissions and NO_3 leaching at different agricultural sites across Europe using LandscapeDNDC. Sci. Total Environ. 553, 128–140.
Nishimura, S., Komada, M., Takebe, M., Yonemura, S., Kato, N., 2012. Nitrous oxide evolved from soil covered with plastic mulch film in horticultural field. Biol. Fert. Soils 48 (7), 787–795.
Nouri, M., Homaee, M., Bannayan, M., Hoogenboom, G., 2017. Towards shifting planting date as an adaptation practice for rainfed wheat response to climate change. Agric. Water Manage. 186, 108–119.
Qin, W., Hu, C., Oenema, O., 2015. Soil mulching significantly enhances yields and water and nitrogen use efficiencies of maize and wheat: a meta-analysis. Sci. Rep. 5, 16210.
Ram, H., Dadhwal, V., Vashist, K.K., Kaur, H., 2013. Grain yield and water use efficiency of wheat (*Triticum aestivum* L.) in relation to irrigation levels and rice straw mulching in North West India. Agric. Water Manage. 128, 92–101.
Ravishankara, A., Daniel, J.S., Portmann, R.W., 2009. Nitrous oxide (N_2O): the dominant ozone-depleting substance emitted in the 21st century. Science 326 (5949), 123–125.
Richardson, C.W., Wright, D.A., 1984. WGEN: A Model for Generating Daily Weather Variables. ARS (USA).
Ruan, H., Feng, P., Wang, B., Xing, H., O'Leary, G.J., Huang, Z., Guo, H., Liu, D.L., 2018. Future climate change projects positive impacts on sugarcane productivity in southern China. Eur. J. Agron. 96, 108–119.
Ruser, R., Flessa, H., Russow, R., Schmidt, G., Buegger, F., Munch, J.C., 2006. Emission of N_2O, N_2 and CO_2 from soil fertilized with nitrate: effect of compaction, soil moisture and rewetting. Soil Biol. Biochem. 38 (2), 263–274.
Smith, K., 2017. Changing views of nitrous oxide emissions from agricultural soil: key controlling processes and assessment at different spatial scales. Eur. J. Soil Sci. 68 (2), 137–155.
Smith, W.N., Grant, B.B., Desjardins, R.L., Rochette, P., Drury, C.F., Li, C., 2008. Evaluation of two process-based models to estimate soil N_2O emissions in Eastern Canada. Can. J. Soil Sci. 88 (2), 251–260.
Smith, W.N., Grant, B.B., Desjardins, R.L., Kroebel, R., Li, C., Qian, B., Worth, D.E.,

McConkey, B.G., Drury, C.F., 2013. Assessing the effects of climate change on crop production and GHG emissions in Canada. Agric. Ecosyst. Environ. 179, 139–150.
Stagnari, F., Galieni, A., Speca, S., Cafiero, G., Pisante, M., 2014. Effects of straw mulch on growth and yield of durum wheat during transition to Conservation Agriculture in Mediterranean environment. Field Crop. Res. 167, 51–63.
Tallec, T., Brut, A., Joly, L., Dumelié, N., Serça, D., Mordelet, P., Claverie, N., Legain, D., Barrié, J., Decarpenterie, T., Cousin, J., Zawilski, B., Ceschia, E., Guérin, F., Le Dantec, V., 2019. N_2O flux measurements over an irrigated maize crop: a comparison of three methods. Agric. For. Meteorol. 264, 56–72.
Taylor, K.E., Stouffer, R.J., Meehl, G.A., 2012. An overview of CMIP5 and the experiment design. Bull. Am. Meteorol. Soc. 93 (4), 485–498.
Tebaldi, C., Knutti, R., 2007. The use of the multi-model ensemble in probabilistic climate projections. Philos. Trans. R. Soc. London, Ser. A 365 (1857), 2053–2075.
Tian, H., Lu, C., Chen, G., Tao, B., Pan, S., Grosso, S.J.D., Xu, X., Bruhwiler, L., Wofsy, S.C., Kort, E.A., Prior, S.A., 2012. Contemporary and projected biogenic fluxes of methane and nitrous oxide in North American terrestrial ecosystems. Front. Ecol. Environ. 10 (10), 528–536.
Walker, S.E., Mitchell, J.K., Hirschi, M.C., Johnsen, K.E., 2000. Sensitivity analysis of the root zone water quality model. Trans. ASAE 43 (4), 841–846.
Wang, Q.X., Fan, X.H., Qin, Z.D., Wang, M.B., 2012. Change trends of temperature and precipitation in the Loess Plateau Region of China, 1961-2010. Global Planet. Change 92-93, 138–147.
Wang, B., Liu, D.L., Asseng, S., Macadam, I., Yu, Q., 2015. Impact of climate change on wheat flowering time in eastern Australia. Agric. For. Meteorol. 209–10, 11–21.
Wang, J., Zhang, Y., Gong, S., Xu, D., Juan, S., Zhao, Y., 2018. Evapotranspiration, crop coefficient and yield for drip-irrigated winter wheat with straw mulching in North China Plain. Field Crop. Res. 217, 218–228.
Wu, X.H., Wang, W., Xie, X.L., Yin, C.M., Hou, H.J., 2018. Effects of rice straw mulching on N_2O emissions and maize productivity in a rain-fed upland. Environ. Sci. Pollut. Res. 25 (7), 6407–6413.
Xiao, D., Tao, F., 2014. Contributions of cultivars, management and climate change to winter wheat yield in the North China Plain in the past three decades. Eur. J. Agron. 52, 112–122.
Xu, C.H., Xu, Y., 2012. The projection of temperature and precipitation over China under RCP scenarios using a CMIP5 multi-model ensemble. Atmos. Oceanic Sci. Lett. 5 (6), 527–533.
Yagioka, A., Komatsuzaki, M., Kaneko, N., Ueno, H., 2015. Effect of no-tillage with weed cover mulching versus conventional tillage on global warming potential and nitrate leaching. Agric. Ecosyst. Environ. 200, 42–53.
Yan, Z., Gao, C., Ren, Y., Zong, R., Ma, Y., Li, Q., 2017. Effects of pre-sowing irrigation and straw mulching on the grain yield and water use efficiency of summer maize in the North China Plain. Agric. Water Manage. 186, 21–28.
Yan, Q., Yang, F., Dong, F., Lu, J., Li, F., Duan, Z., Zhang, J., Lou, G., 2018. Yield loss compensation effect and water use efficiency of winter wheat under double-blank row mulching and limited irrigation in northern China. Field Crop. Res. 216, 63–74.
Yi, Y., 2009. Research Methods of Soil Physics. Peking University Press, Beijing, China (in Chinese).
Yu, Y., Tao, H., Jia, H., Zhao, C., 2017. Impact of plastic mulching on nitrous oxide emissions in China's arid agricultural region under climate change conditions. Atmos. Environ. 158, 76–84.
Yu, Y., Tao, H., Yao, H., Zhao, C., 2018. Assessment of the effect of plastic mulching on soil respiration in the arid agricultural region of China under future climate scenarios. Agric. For. Meteorol. 256-257, 1–9.
Zhang, Y., Niu, H., 2016. The development of the DNDC plant growth sub-model and the application of DNDC in agriculture: a review. Agric. Ecosyst. Environ. 230, 271–282.
Zhang, Y., Li, C.S., Zhou, X.J., Moore, B., 2002. A simulation model linking crop growth and soil biogeochemistry for sustainable agriculture. Ecol. Modell. 151 (1), 75–108.
Zhang, Y., Niu, H., Wang, S., Xu, K., Wang, R., 2016. Application of the DNDC model to estimate N_2O emissions under different types of irrigation in vineyards in Ningxia, China. Agric. Water Manage. 163, 295–304.
Zhang, F., Zhang, W., Li, M., Zhang, Y., Li, F., Li, C., 2017. Is crop biomass and soil carbon storage sustainable with long-term application of full plastic film mulching under future climate change? Agric. Syst. 150, 67–77.
Zhang, F., Zhang, W., Qi, J., Li, F.-M., 2018a. A regional evaluation of plastic film mulching for improving crop yields on the Loess Plateau of China. Agric. For. Meteorol. 248, 458–468.
Zhang, J., Balkovič, J., Azevedo, L.B., Skalský, R., Bouwman, A.F., Xu, G., Wang, J., Xu, M., Yu, C., 2018b. Analyzing and modelling the effect of long-term fertilizer management on crop yield and soil organic carbon in China. Sci. Total Environ. 627, 361–372.